www.nature.com/mi

MucosalImmunology

ARTICLE

High expression of Sonic hedgehog in allergic airway epithelia contributes to goblet cell metaplasia

Chengyun Xu[1,2], Chaochun Zou[3], Musaddique Hussain[1,2], Wei Shi[1,2], Yanan Shao[3], Ziyan Jiang[3], Xiling Wu[3], Meiping Lu[3], Junsong Wu[4], Qiangmin Xie[1,2], Yuehai Ke[5], Fanxin Long[6], Lanfang Tang[3] and Ximei Wu[1,2]

Sonic hedgehog (SHH) is abundantly expressed and critical for morphogenesis in embryonic lungs; however, SHH expression drops to a much lower level in mice from E17.5 and in humans from the 21st gestational week. We find that SHH expression is robustly upregulated in the airway epithelia of children with asthma or mouse models with allergic airway disease. Specifically, airway-specific SMO loss of function significantly suppresses allergen-induced goblet cell phenotypes, whereas an airway-specific SMO gain of function markedly enhances the goblet cell phenotypes in mouse models with allergic airway disease. Notably, intratracheal administration with SHH-neutralizing antibody or cyclopamine robustly attenuates goblet cell phenotypes in mouse models with allergic airway disease. Finally, we identify that *Muc5AC* gene encoding MUC5AC mucin serves as a direct target of GLI transcriptional factors in response to SHH, whereas the SAM-pointed domain-containing ETS transcription factor and Forkhead box A2, critical transcriptional factors for goblet cell phenotypes, both function as the effectors of GLIs in response to SHH stimulation. Together, the upregulation of SHH expression in allergic bronchial epithelia contributes to goblet cell metaplasia; thus, blockage of SHH signaling is a rational approach in a therapeutic intervention of epithelial remodeling in chronic airway diseases.

Mucosal Immunology (2018) 11:1306–1315; https://doi.org/10.1038/s41385-018-0033-4

INTRODUCTION

Mucous cell metaplasia, defined as the reversible transformation of airway epithelia to mucous cells, occurs in many chronic airway diseases, such as asthma, cystic fibrosis, and chronic obstructive pulmonary disease (COPD). It is characterized by mucous hypersecretion and associated with the morbidity and mortality of these pathological conditions.[1] In mucous cell metaplasia of airway epithelia, increases in goblet cell numbers and decreases in Club cell and ciliated cell numbers have been thought to result from the transition of Club cells and ciliated cells to goblet cells.[2,3] Among a variety inflammatory mediators, interleukin-13 (IL-13) orchestrated with epidermal growth factor is believed to be extremely critical for Th2 cell-induced goblet cell metaplasia, by binding to IL-13 receptor and subsequent signal transducer and activator of transcription 6 activation.[3,4] IL-13 induces the expression of not only *Muc5AC*—the gene leading to mucin synthesis, a defining characteristic of the goblet cell phenotype—but also of critical transcriptional factor genes including *forkhead box A2* (*FoxA2*) and *SAM-pointed domain-containing ETS transcription factor* (*Spdef*).[5–7] FOXA2 is required for maintenance of the normal differentiation of airway epithelium, and the inhibition of FOXA2 appears to be an important early step in initiation of goblet cell metaplasia.[7,8] SPDEF has been shown to be both necessary and sufficient to induce a transcriptional program that results in goblet cell metaplasia.[6,9]

The mammalian hedgehog (HH) family of secreted proteins consists of Sonic hedgehog (SHH), Indian hedgehog (IHH), and Desert hedgehog (DHH).[10] SHH is translated as a ~45 kD precursor and it undergoes autocatalytic processing to produce a ~20 kD N-terminal signaling domain (N-SHH) and a ~25 kD C-terminal domain with no known signaling role.[10] In the presence of SHH, the binding of SHH to PTCH1 relieves the inhibition of SMO, thereby activating GLI transcriptional factors (GLI1 and GLI2) and inducing the transcription of target genes including *Cyclin D*, *Cyclin E*, *Myc*, as well as *patched 1* (*PTCH1*) and *GLI family zinc finger 1* (*GLI1*).[11,12] In embryonic lungs, since SHH is expressed in the distal epithelium and PTCH1 is expressed in the juxtaposed mesenchyme, SHH is believed to directly signal mesenchymes in a paracrine fashion.[13] Overexpression of SHH leads to increased epithelial and mesenchymal cell proliferation, resulting in the formation of lungs with overly abundant mesenchymes and no functional alveoli;[14] in SHH knockout, on the other hand, it manifests as significant defects in branching morphogenesis, resulting in the formation of rudimentary respiratory organs with a few large, poorly vascularized airways.[13,15] However, SHH produced by lung epithelium actively maintains adult lung quiescence and epithelia-specific deletion of SHH results in a proliferative expansion of the adjacent lung mesenchyme.[16]

Despite the abundance of SHH in early-stage embryonic lungs, SHH expression in lungs drops to a greatly lower level in mice

[1]Department of Pharmacology, Zhejiang University School of Medicine, 310058 Hangzhou, China; [2]Key Laboratory of CFDA for Respiratory Drug Research, Zhejiang University School of Medicine, 310058 Hangzhou, China; [3]Department of Respiratory Medicine of the Children's Hospital, Zhejiang University School of Medicine, 310058 Hangzhou, China; [4]Department of Orthopedics of the First Affiliated Hospital, Zhejiang University School of Medicine, 310058 Hangzhou, China; [5]Department of Pathology, Zhejiang University School of Medicine, 310058 Hangzhou, China and [6]Departments of Orthopedics, Medicine and Developmental Biology, Washington University in St. Louis, St. Louis, MO 63110, USA

Correspondence: Lanfang Tang (6195007@zju.edu.cn) or Ximei Wu (xiwu@zju.edu.cn)

These authors contributed equally: Chengyun Xu, Chaochun Zou.

Received: 7 August 2017 Revised: 15 March 2018 Accepted: 27 April 2018
Published online: 4 June 2018

from E17.5 and in humans from the 21st gestational week.[17,18] Although the results of immunohistochemical staining indicate that SHH and GLI1 are undetectable in airway of normal adult mouse,[19] *SHH*^{creGFP} reporter mice show that SHH is expressed in adult lung epithelia, predominantly in the Scgb1a1^{+} club epithelial cells in the proximal airway, with scattered expression in ciliated epithelium and the Sftpc^{+} alveolar type II epithelial cells.[16]

In the present study, we investigate SHH expression in allergic airways and explore its implications. We reveal that SHH is highly expressed in the airway epithelia of both children with asthma and mouse models with allergic airway disease, and that the upregulation of SHH expression essentially contributes to bronchial goblet cell metaplasia and mucous hypersecretion.

RESULTS

High expression of SHH in airway epithelia of children with asthma and mouse models with allergic airway disease

To determine the SHH expression pattern in airway epithelia, broncho-alveolar lavage fluids (BALFs) from children with allergic asthma or foreign body aspiration (FBA) were prepared for cytospin and ELISA determination of N-SHH, an active form of SHH. The results of Wright-Giemsa staining indicated that eosinophils typically existed in large number in the BALFs of children with asthma, but not in those with FBA (Supplementary Fig. 1a). Immunostaining results indicated that both SHH and Club cell 10 kDa protein (CC10)-derived immune signals were robustly detectable, an apparent overlapping signal was readily observed in the BALF cells of children with asthma, but not in those with FBA (Fig. 1a). Finally, the results of the ELISA assay for BALF supernatants indicated that N-SHH was significantly increased in the BALFs of children with asthma, compared to those with FBA (Fig. 1b).

We next generated mouse models with allergic airway disease to investigate the expression patterns of HH ligands, by sensitizing and challenging the adult mice with either ovalbumin (OVA) or house dust mite (HDM). Each of the OVA or HDM challenge led to a significant infiltration of inflammatory cells, especially eosinophils, into the peribronchial and perivascular tissues of lungs and an apparent metaplasia of bronchial epithelia (Fig. 1c, f). SHH was expressed at an almost undetectable level in the lungs of control mice, but at a robust level in both the bronchial and alveolar epithelia in the lungs of either OVA or HDM-challenged mice (Fig. 1c, f). Although DHH expression was almost undetectable in lungs and IHH was apparently expressed in the alveolar and bronchial epithelia and the peribronchial tissues, the expression patterns of both DHH and IHH were not affected by OVA challenge (Supplementary Fig. 1b, c). Consistently, OVA challenge increased SHH mRNA and protein levels in turn, but induced neither mRNA nor protein of DHH and IHH (Fig. 1d, e; Supplementary Fig. 1d, e). Thus, SHH expression is significantly upregulated in the airway epithelia of not only mouse models with allergic airway disease, but also children with allergic asthma.

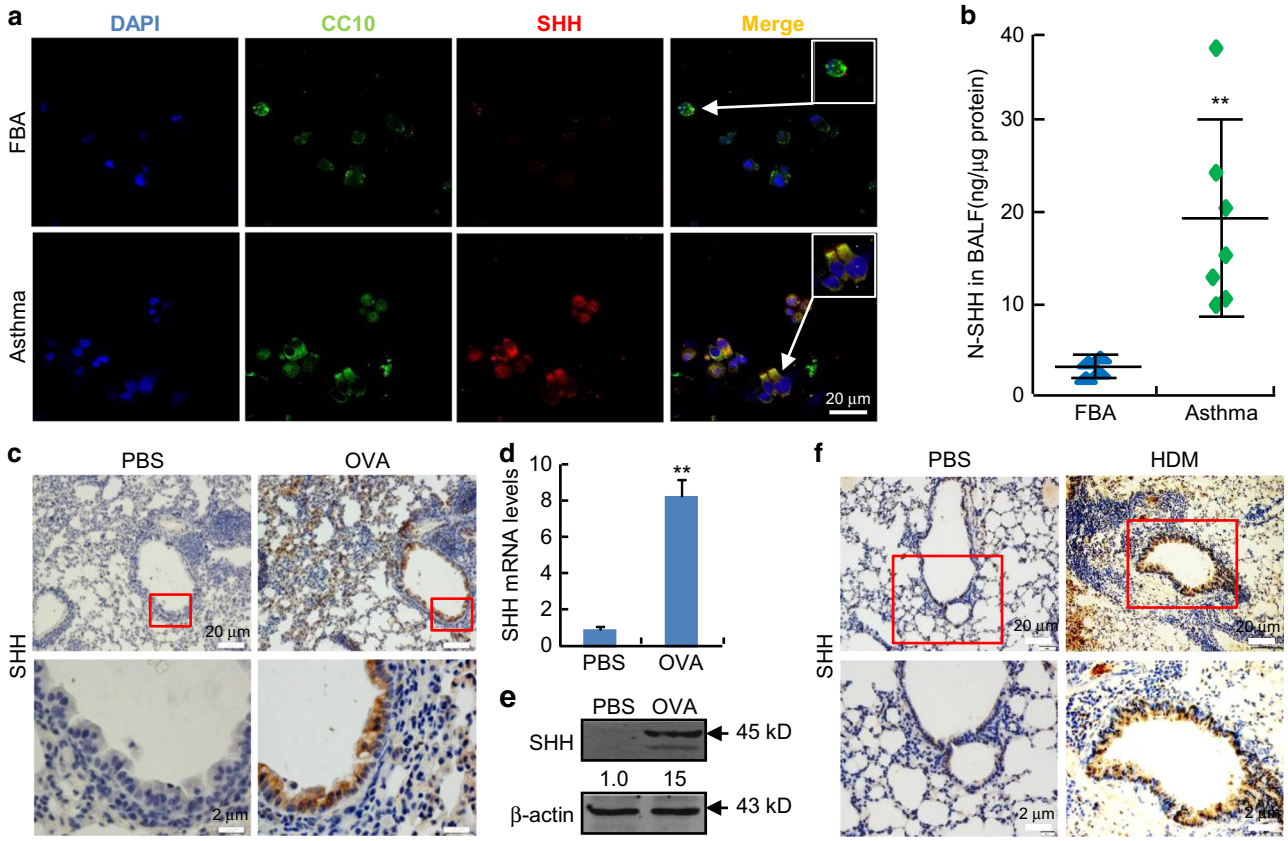

Fig. 1 SHH expression in bronchial epithelia of children with asthma and mouse models with allergic airway disease. **a**, **b** BALF cytospins from children with FBA or asthma were used for immunostains of CC10, SHH, and DAPI (**a**), and BALF supernatants were used for ELISA determination of N-SHH and protein quantification (**b**). **c**–**e** OVA-sensitized mice were aerosolized with 1% OVA or an equal volume of PBS for 30 min once, daily for 7 days. Lungs were subjected to paraffin-embedded sectioning, RNA isolation, and the preparation of cell lysates for immunostaining (**c**), quantitative RT-PCR (**d**), and Western blotting (**e**), respectively. **f** HDM-sensitized mice were intranasally challenged with HDM or an equal volume of PBS once daily for 3 days. Lungs were subjected to paraffin-embedded sectioning and immunostaining for SHH. $^{**}p < 0.01$ vs. PBS challenge (each $n = 6$) or vs. children with FBA ($n = 4$ for FBA and $n = 7$ for asthma). Square frames define the magnified regions

Attenuation of allergen-induced goblet cell metaplasia by SHH-neutralizing antibody or cyclopamine

To investigate the implication of SHH upregulation, the mice were received an intratracheal instillation of N-SHH-neutralizing antibody (SHH-Nab) at 0.5 or 2.0 μg/mouse, 2 h after each OVA aerosolization, once daily for 7 days. The total inflammatory cell numbers in BALFs increased significantly after OVA challenge, among macrophages (Mac), lymphocytes (Lym), eosinophils (Eos), and neutrophils (Neu), eosinophils most strikingly increased, up to 58-fold (Fig. 2a). SHH-Nab significantly attenuated the number of inflammatory cells, including macrophages and eosinophils, and the infiltration into peribronchial and perivascular connective tissues in a dose-dependent manner in OVA-challenged mice (Fig. 2a, b). OVA challenge also prompted the apparent activation of HH signaling in bronchial epithelia, exhibiting an increased expression of PTCH1 (a target of HH signaling), whereas SHH-Nab at 0.5 or 2.0 μg/mouse dose dependently attenuated PTCH1 expression (Fig. 2c and Supplementary Fig. 2a). In correlation with its attenuation of HH signaling, SHH-Nab dose dependently suppressed OVA-induced Periodic Acid-Schiff (PAS) and MUC5AC staining areas in bronchial epithelia (Fig. 2c and Supplementary Fig. 2a). Finally, the specificity of SHH-Nab in attenuating the allergen-induced activation of HH signaling and the goblet cell metaplasia was further confirmed through the use of recombinant mouse N-SHH protein (rmN-SHH) as an immunogen of SHH-Nab. Recombinant mouse N-SHH protein robustly reversed SHH-Nab-negated PTCH1 expression, and also the PAS and MUC5AC staining areas (Supplementary Fig. 3). Thus, the high expression of SHH contributes to the activation of HH signaling and goblet cell phenotypes in the bronchial epithelia of a mouse model with allergic airway disease.

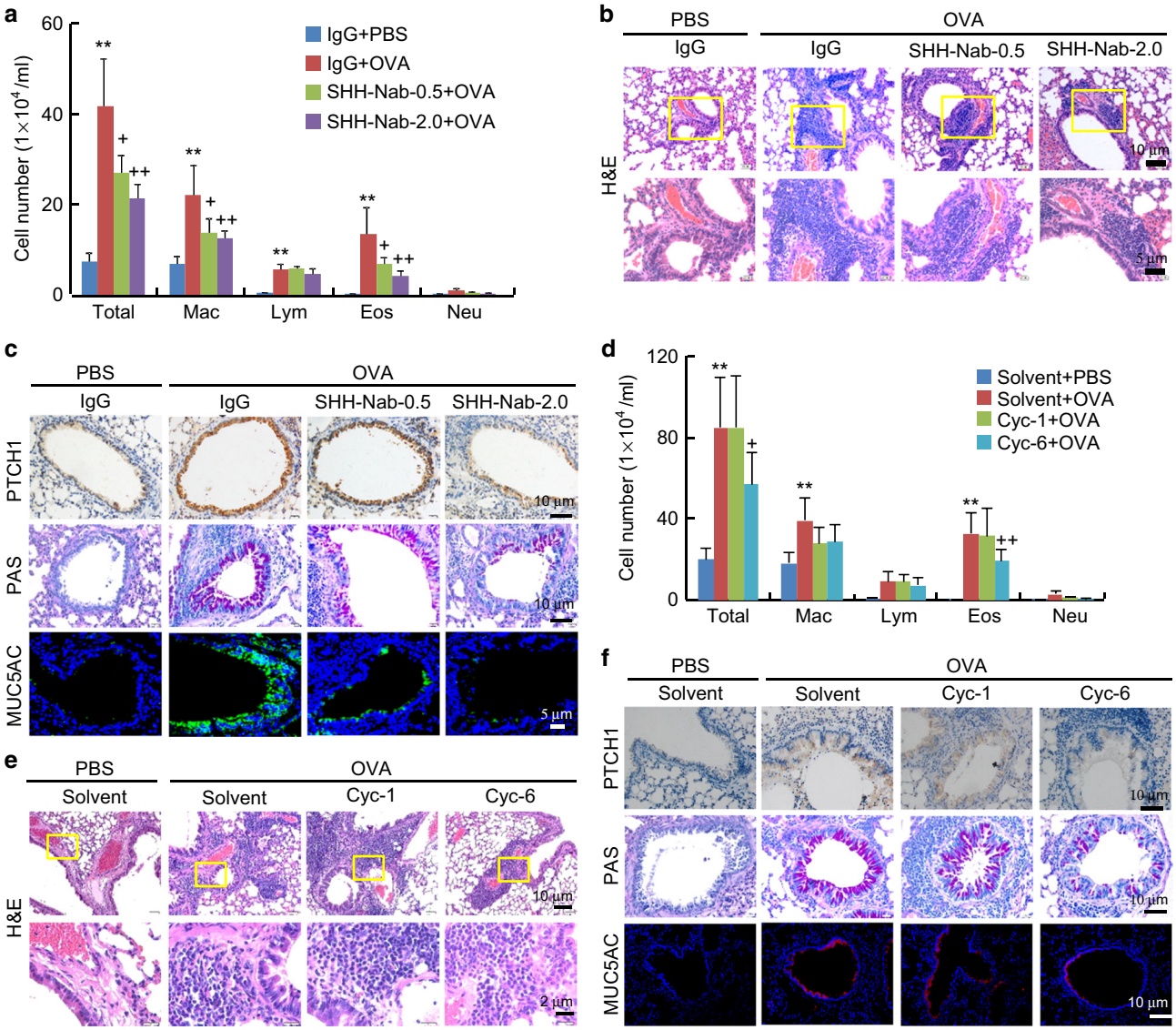

Fig. 2 Attenuation of bronchial goblet cell phenotypes by SHH neutralizing antibody or cyclopamine in a mouse model with allergic airway disease. OVA-sensitized mice were aerosolized with 1% OVA or an equal volume of PBS for 30 min, once daily for 7 days. Two hours after each OVA challenge, mice were intratracheally administered 50μl/mouse of SHH neutralizing antibody (SHH-Nab) at 10 and 40 μg/ml (**a**–**c**) or aerosolized with 5 ml of cyclopamine solution at 1 and 6 mg/ml for 15 min, once daily for 7 days (**d**–**f**); the control mice were intratracheally administered with same volume of solvent. Twenty-four hours after the last OVA challenge, BALFs were prepared for cell counting and classification (**a**, **d**), whereas lungs were subjected to paraffin-embedded sectioning for H&E staining (**b**, **e**), PAS staining (**c**, **f**), and immunostaining for PTCH1 and MUC5AC (**c**, **f**). Each $n = 6$. $^{**}p < 0.01$ vs. IgG/solvent treatment and PBS challenge; $^{+}p < 0.05$; $^{++}p < 0.01$ vs. IgG/solvent treatment and OVA challenge. Square frames define the magnified regions

To determine whether goblet cell metaplasia by aberrant SHH in airway epithelia indeed results from activation of HH signaling, we inhibited SMO activity in bronchial epithelia via the aerosol administration of a SMO inhibitor, cyclopamine (Cyc.), into mice 2 h after each OVA challenge; we then evaluated the inflammatory cell infiltration and goblet cell phenotypes. The number of inflammatory cells in BALFs, especially eosinophils, had significantly increased; on the other hand, cyclopamine at 6 mg/ml significantly reduced the total number of inflammatory cells and eosinophils, and cyclopamine at 1 mg/ml did not affect the OVA-induced accumulation of inflammatory cells (Fig. 2d, e). OVA challenge caused the increases in PTCH1, PAS, and MUC5AC staining in bronchial epithelia; cyclopamine at 1 and 6 mg/ml dose dependently attenuated OVA-induced PTCH1 and MUC5AC expression, as well as PAS staining (Fig. 2f and Supplementary Fig. 2b). Thus, the neutralization of N-SHH or the inhibition of SMO activity is sufficient in suppressing the allergen-induced HH signaling activation in bronchial epithelia and subsequently blocking goblet cell metaplasia.

Effects of SMO loss or gain of function in allergen-induced goblet cell metaplasia

To investigate the specific roles of aberrant activation of HH signaling in bronchial goblet cell metaplasia, we disrupted *SMO* via the intratracheal instillation of adenoviruses expressing *Cre recombinase* and green fluorescent protein (*GFP*) into $SMO^{flox/flox}$ mice, 3 days before OVA challenge; an OVA challenge was then performed once daily, for a total of 7 days. The knockout efficiency of SMO in bronchial epithelia, mesenchymal stromal cells, and eosinophils were examined in lung single-cell suspensions of OVA-challenged $SMO^{flox/flox}$ mice with infection of either GFP-expressing or Cre-expressing adenoviruses. The results from immunofluorescent staining determined that Cre-expressing adenoviruses almost completely abolished the SMO expression in CC10-positive cells (Club cells), but had no apparent effect on SMO expression in either vimentin-positive cells (mesenchymal stromal cells) or C-C chemokine receptor type 3 (CCR3)-positive cells (eosinophils), in comparison to GFP-expressing adenoviruses (Supplementary Fig. 4). OVA challenge resulted in significant increases in the numbers of macrophage, lymphocytes, eosinophils, and neutrophils in BALFs; the intratracheal instillation of adenoviruses-expressing Cre or GFP alone resulted in no apparent changes in the total numbers of inflammatory cells and classification in BALFs, of either PBS or OVA-aerosolized $SMO^{flox/flox}$ mice (Fig. 3a, b). SMO was predominantly expressed in alveolar and bronchial epithelia in PBS-challenged lungs, and in OVA-challenged lungs was robustly expressed in not only airway epithelia but also inflammatory cells (Fig. 3c, f). Specifically, Cre-expressing adenoviruses significantly reduced SMO expression in bronchial epithelia, but not inflammatory cells in either PBS or OVA-challenged $SMO^{flox/flox}$ mice, compared to GFP-expressing adenoviruses (Fig. 3c; Supplementary Fig. 2c, d). Most strikingly, in OVA-challenged mice, the expression of Cre in bronchial epithelia almost completely abolished the increases in PAS-positive areas, compared to the expression of GFP; likewise, in OVA-challenged bronchial epithelia, the expression of Cre markedly diminished the increases in MUC5AC-derived and PTCH1-derived immune signals (Fig. 3c and Supplementary Fig. 2d). Thus, the SMO loss of function in bronchial epithelia attenuates the allergen-induced HH signaling activation and goblet cell metaplasia as well.

To investigate whether the activation of SMO suffices in inducing goblet cell phenotypes in mice challenged with an allergen, we overexpressed the constitutively active form of SMO (SMO-M2, SMO-W539L) in airway epithelia by intratracheally instilling Cre-expressing adenoviruses into *R26-SMO-M2* mice, 3 days before OVA challenge. The OVA challenge was performed once daily for only 3 days, to induce a mild airway inflammation (Fig. 3d, e). Cre-expressing adenoviruses markedly increased SMO and PTCH1 expression in the bronchial epithelia of either PBS-challenged or OVA-challenged *R26-SMO-M2* mice and slightly induced the PAS-staining and MUC5AC-staining areas in the bronchial epithelia of PBS-challenged *R26-SMO-M2* mice; but Cre-expressing adenoviruses led to significant increases in PAS and MUC5AC-staining areas in comparison to GFP-expressing adenoviruses in OVA-challenged *R26-SMO-M2* mice (Fig. 3f and Supplementary Fig. 2e). Thus, the constitutive activation of SMO in bronchial epithelia suffices in inducing apparent goblet cell phenotypes in a mouse model with mild allergic airway disease.

Underlying mechanisms governing SHH-induced goblet cell metaplasia

To explore the potential involvement of GLI1 and GLI2 in SHH-induced goblet cell metaplasia, we cultured human bronchial epithelial cells, 16HBE. Purmorphamine (Purm.), a SMO agonist, increased the mRNA levels of not only *PTCH1* but also *Muc5AC* in a dose-dependent manner (Fig. 4a). Likewise, purmorphamine at 5 μM increased the *Muc5AC* promoter-driven luciferase activity (Fig. 4b). The specificity was further confirmed by the SHH recombinant protein N-SHH, which at 200 ng/ml significantly increased the luciferase activity (Fig. 4c). To investigate the role of GLI transcriptional factors in the SHH-induced transactivation of *Muc5AC*, we knocked down the GLI1 and GLI2, activators of HH signaling, via their respective shRNA-expressing lentiviruses in 16HBE cells; we then performed quantitative RT-PCR. Purmorphamine at 5 μM increased *Muc5AC* mRNA levels, whereas either GLI1 or GLI2 knockdown attenuated purmorphamine-induced *Muc5AC* mRNA levels by 70–80% (Fig. 4d). Conversely, the overexpression of GLI2 increased the *Muc5AC* luciferase activity by 0.6-fold, whereas overexpression of N-terminally truncated GLI2 (a constitutively active form of GLI2, ΔN-Gli2) induced the luciferase activity up to 2.5-fold (Fig. 4e). To determine the physical interaction between GLI2 and the promoter region of *Muc5AC* gene, we performed ChIP-PCR in 16HBE cells by using antibody against GLI2 and a negative control IgG. As expected, GLI2 apparently bound to the DNA fragment of *Muc5AC* gene, compared to IgG (Fig. 4f). Thus, *Muc5AC* serves as a downstream target gene of GLI transcriptional factors in response to SHH.

To determine whether SHH-induced goblet cell metaplasia is associated with FOXA2 and SPDEF, the critical transcriptional factors for goblet cell phenotypes, we also analyzed FOXA2 and SPDEF expression in 16HBE cells and in SMO-deficient or SMO-activated bronchial epithelia. Purmorphamine ranging from 0 to 5 μM, or N-SHH recombinant protein ranging from 0 to 200 ng/ml, dose dependently induced SPDFE mRNA and protein levels but reduced FOXA2 mRNA and protein levels (Fig. 4g, h). Moreover, cyclopamine ranging from 0 to 10 μM dose dependently reversed not only N-SHH-negated FOXA2 expression but also N-SHH-induced SPDFE expression; additionally, cyclopamine at 10 μM not only completely reversed FOXA2 and SPDEF expression, but also reduced the basal levels of SPDEF (Fig. 4i). In addition, the knockdown of GLI1 and GLI2 by their respective shRNA-expressing lentiviruses reduced the SPDEF mRNA levels, but increased the FOXA2 mRNA levels, in the absence of purmorphamine (Fig. 4j). In the presence of purmorphamine, knockdown of GLI1 reversed purmorphamine-induced SPDEF mRNA levels by 60% and purmorphamine-negated FOXA2 mRNA levels by 30%, whereas the knockdown of GLI2 reversed purmorphamine-induced SPDEF mRNA levels by 65% and purmorphamine-negated FOXA2 mRNA levels by 130% (Fig. 4j).

To determine the expression of FOXA2 and SPDEF in response to HH signaling in vivo, we performed Western blotting on lung tissues and immunostaining assays on bronchial epithelia. In the lungs of $SMO^{flox/flox}$ mice, Cre-expressing adenoviruses increase FOXA2 and decreased SPDEF protein levels in the absence of OVA challenge; OVA challenge, rather, led to an 80% decrease in FOXA2 protein and a 140% increase in SPDEF protein. On the

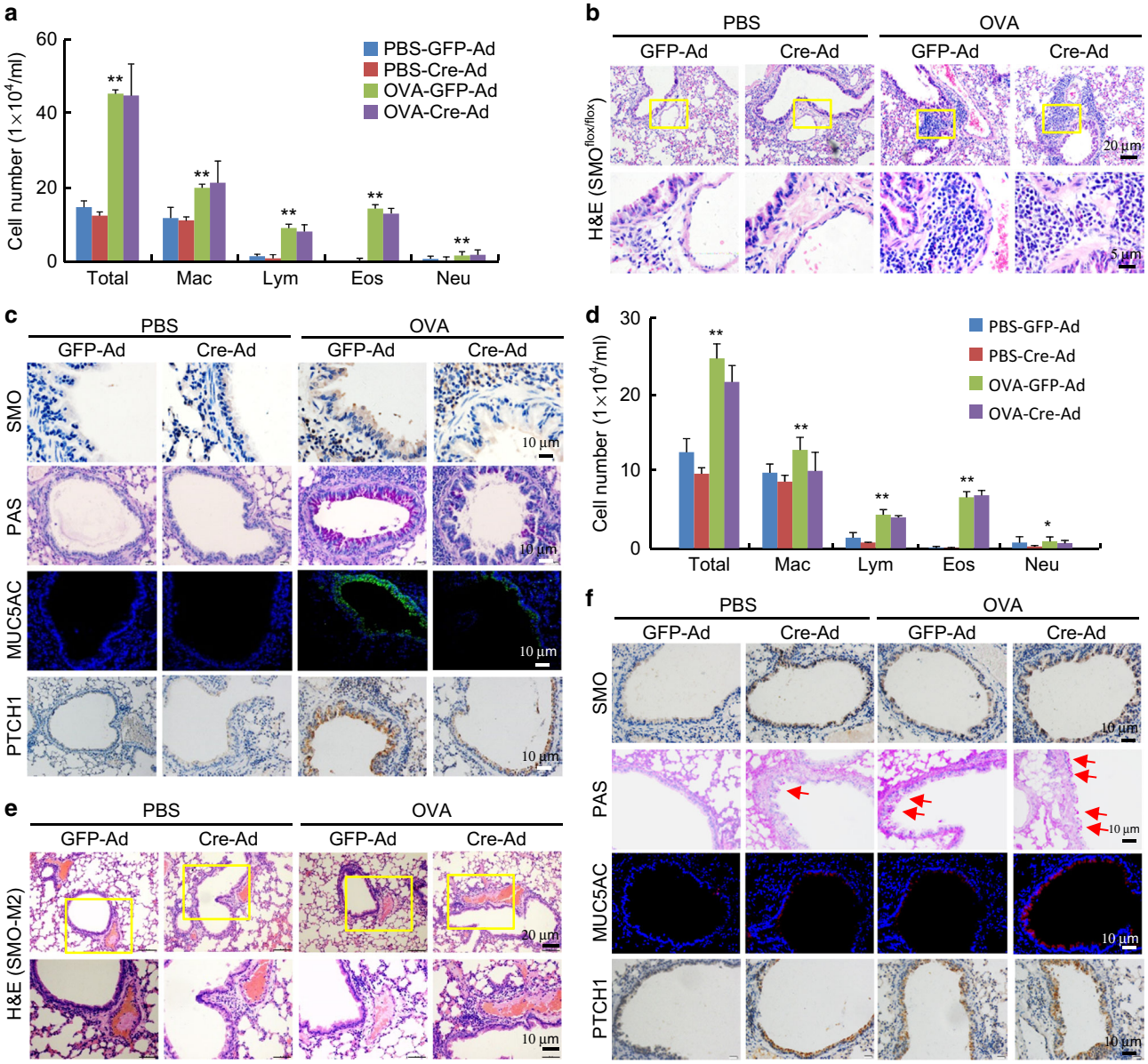

Fig. 3 Effects of SMO loss of function and gain of function in bronchial epithelia on goblet cell phenotypes of a mouse model with allergic airway disease. OVA-sensitized *SMO*$^{flox/flox}$ and *R26-SMO-M2* mice were intratracheally instilled with GFP-expressing or Cre-expressing adenoviruses with titer of 2×10^6 PFU at volume of 50 μl/mouse once daily for 3 days; then, mice were aerosolized with 1% OVA or an equal volume of PBS for 30 min, once daily for 7 days (*SMO*$^{flox/flox}$ mice, **a**–**c** or 3 days (*R26-SMO-M2* mice, **d**–**f**)). Twenty-four hours after the last OVA challenge, BALF cytospins were prepared for cell counting and classification (**a**, **d**), and lungs were subjected to paraffin-embedded sectioning for H&E staining (**b**, **e**), PAS staining (**c**, **f**), and immunostaining for SMO, PTCH1, and MUC5AC (**c**, **f**). Each $n = 6$. $^{**}p < 0.01$ vs. PBS challenge and infection with GFP-expressing adenoviruses. Square frames define the magnified regions

other hand, Cre-expressing adenoviruses completely reversed not only OVA-negated FOXA2 protein but also OVA-induced SPDEF protein (Fig. 4k). Immunofluorescence assays consistently revealed that OVA challenge in GFP-expressing bronchial epithelia led to the apparent diminishment of FOXA2-derived immune signals but robust enhancement of SPDEF-derived immune signals; nonetheless, Cre-expressing adenoviruses significantly reversed not only OVA-negated FOXA2-derived immune signals but also OVA-induced SPDEF-derived immune signals (Fig. 4l, m). Moreover, the results of Western blotting indicated that SHH-Nab dose dependently reversed the expression of OVA-negated FOXA2 and OVA-induced SPDEF (Supplementary Fig. 5a). In *R26-SMO-M2* mice, the results of both Western blotting and immunostaining assays indicated that OVA challenge in GFP-expressing bronchial epithelia led to the apparent diminishment of FOXA2 expression but the marked enhancement of SPDEF expression; notably, Cre-expressing adenoviruses further reduced OVA-negated FOXA2 expression but potentiated OVA-induced SPDEF expression (Supplementary Fig. 5b–d). Collectively, SHH induces goblet cell metaplasia possibly through the upregulation of SPDEF expression and the downregulation of FOXA2 expression in bronchial epithelia.

DISCUSSION

The present study, to the best our knowledge, is the first to reveal that high expression of SHH in Club cells autocrinely/paracrinely activates HH signaling, and thus induce goblet cell metaplasia in

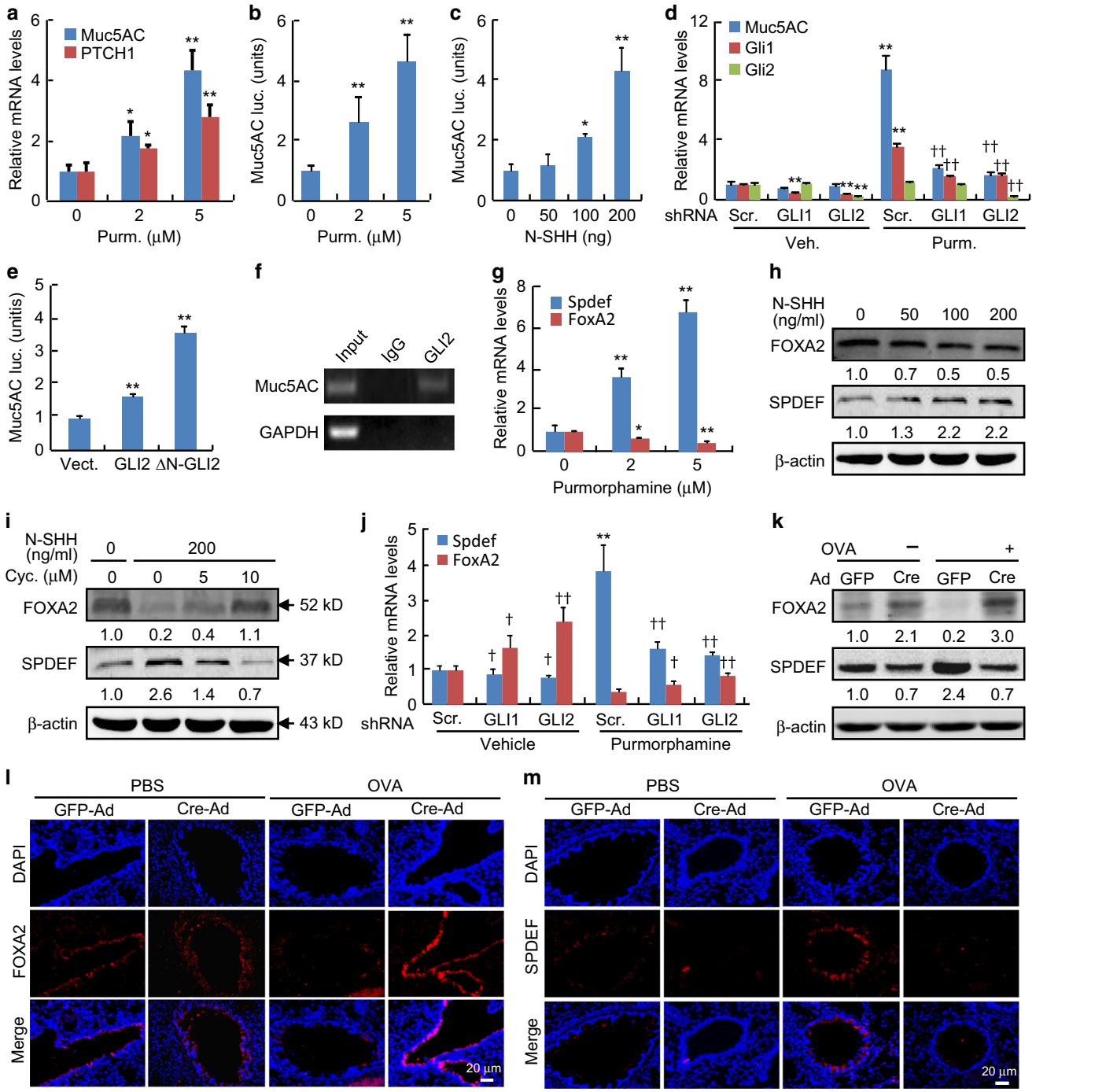

Fig. 4 Mechanisms underlying SHH-induced goblet cell metaplasia. **a**–**e** 16HBE cells were subjected to quantitative RT-PCR and *Muc5AC* luciferase assays, 24 and 36 h after the treatments with indicated concentrations of purmophamine (Purm.)/N-SHH (or 5 μM purmophamine), respectively. In some cases, cells were infected with scramble (Scr.)-expressing, GLI1-expressing, or GLI2-shRNA-expressing lentiviruses, or transfected with *Muc5AC* reporter, vector, GLI2, or ΔN-GLI2, 24 h before purmophamine treatments. **f** ChIP-PCR assays were performed in 16HBE cells by using GLI2 antibody and a negative control IgG. **g**–**j** 16HBE cells were treated with indicated concentrations of purmophamine or N-SHH, for 24 h. In some cases, cells were infected with scramble-expressing, GLI1-expressing, or GLI2-shRNA-expressing lentiviruses 24 h before purmophamine treatments, or pretreated with indicated concentrations of cyclopamine 3 h before and during purmophamine treatments. Cells were then subjected to quantitative RT-PCR (**g**, **j**) and Western blotting (**h**, **i**). **k**–**m** Western and immunohistochemistry assays for FOXA2 and SPDEF expression in $SMO^{flox/flox}$ mice intratracheally instilled with GFP-expressing or Cre-expressing adenoviruses and challenged with OVA or PBS. Each $n = 4$. $^{*}p < 0.05$, $^{**}p < 0.01$ vs. 0 μM purmorphamine, 0 ng/ml N-SHH, scramble-shRAN and vehicle treatments, or vector transfection; $^{++}p < 0.01$ vs. scramble-shRAN and purmorphamine treatments

the bronchi of mouse models with allergic airway disease, and possibly those of children with allergic asthma. In this molecular event, the binding of SHH to PTCH1 relieves the inhibition of SMO and subsequently activates GLI transcriptional factors, thereby inducing the transcription of mucin genes, such as *Muc5AC*. In addition, the activation of GLI transcriptional factors by SHH upregulates SPDEF and downregulates FOXA2 expression in bronchial epithelia to induce goblet cell metaplasia (Fig. 5).

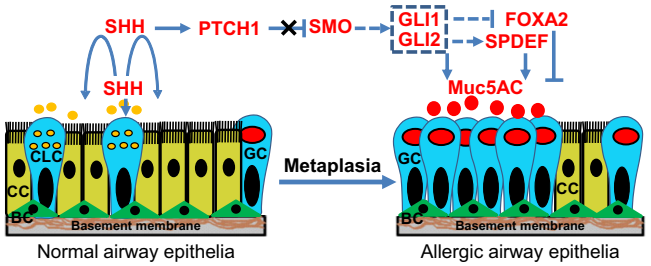

Fig. 5 A model of the role of SHH in the goblet cell metaplasia of allergic airway epithelia. In allergic airway epithelia, SHH secreted from Club cells autocrinely/paracrinely activates HH signaling, to induce the mucin gene (e.g., *Muc5AC*) expression, upregulate SPDEF expression, and downregulate FOXA2 expression, resulting in the goblet cell metaplasia and mucous hypersecretion. CC ciliated cell, CLC club cell, GB goblet cell, BC basal cell

SHH is abundant in both the bronchial and respiratory epithelia of early-stage embryonic lungs,[13–15,20] albeit at a greatly lower level in mice from E17.5 and in humans from the 21st gestational week.[17,18] Consistent with these findings, both the present study and the literature indicate that SHH is expressed at almost undetectable levels in the bronchial epithelia of normal adult mice.[19] However, SHH^{creGFP} reporter mice show that SHH is abundantly expressed in the adult lung epithelium predominantly in the Scgb1a1^{+} Club cells in the proximal airway, with scattered expression in ciliated epithelium.[16] The discrepancy could be explained by the fact that the approach of reporter mice is much more sensitive than that of immunohistochemistry staining in detecting the expression of SHH in adult mouse airways. Despite the low levels of SHH in normal adult airways, SHH is strikingly upregulated in bronchial epithelia of not only mouse models with allergic airway disease, but also those of children with asthma. Consistent with our findings, previous studies have shown that upregulation of SHH occurs in airway epithelia of a mouse model with allergic airway disease, fluorescein isothiocyanate (FITC)-induced lung fibrosis, or naphthalene-induced lung injury, and in patients with idiopathic pulmonary fibrosis.[19,21–25] Inconsistent with these findings, previous study indicates that both acute and chronic naphthalene-induced lung injury cause a reduction in SHH expression and HH signaling activation, as assessed through decreased SHH^{creGFP} reporter activity in airway epithelia and $Gli1^{LacZ}$ reporter activity in the mesenchyme surrounding the airway.[16]

In conducting airways of embryonic lungs, the expression pattern of SHH is consistent with the distribution of nonciliated bronchiolar cells (i.e., Club cells) and the Club cell marker, CC10.[22,26] In adult SHH^{creGFP} reporter mice, SHH is predominantly expressed in Scgb1a1^{+} Club cells in the proximal airway, with scattered expression in ciliated epithelium.[16] Likewise, the upregulation of SHH co-occurs with CC10 expression in FITC-induced murine pulmonary inflammation.[22] It is believed that nonciliated bronchiolar cells are the SHH-producing cells, and ciliated bronchiolar cells and epithelial progenitors are the HH-responding cells.[19,22,26] Since HH ligands signal through both autocrine and paracrine mechanisms to regulate cell function and differentiation,[12,19,27] we suppose that in allergic airway epithelia, SHH secreted by nonciliated bronchiolar cells acts upon ciliated bronchiolar cells or airway epithelial progenitors to transform into goblet cells. The mechanism underlying the upregulation of SHH in allergic bronchial epithelia remains unknown. Nuclear factor-κB (NF-κB) contributes to the overexpression of SHH and activation of HH signaling in pancreatic cancer.[28] Given the fact that allergen induces a variety of proinflammatory cytokines capable of activating NF-κB signaling in asthma,[29] we speculate that the upregulation of SHH expression in allergic airway epithelia possibly results from activation of NF-κB signaling.

T helper 2 (Th2) cytokines play a key role in promoting goblet cell metaplasia in asthma. The direct involvement of IL-4, IL-9, and IL-13 in goblet cell metaplasia and mucous hypersecretion has been substantiated in animal models.[30–32] Among them, IL-13 and IL-4 are considered as the prime effector molecules that induce goblet cell metaplasia.[30] Although previous studies propose that SHH production and GLI signaling are activated in lung to enhance the Th2 response during a mouse model of allergic airway disease—and that IL-4, a Th2 cytokine, is a novel transcriptional target of HH signals in T cells[23,25]—the contribution of SHH in goblet cell differentiation of allergic bronchial epithelia is confirmed in the present study; this indicates that either the neutralization of SHH by SHH-Nab or the disruption of SMO in bronchial epithelial attenuates allergen-induced goblet cell metaplasia, whereas activation of SMO enhances allergen-induced goblet cell metaplasia. Though inhibition of SMO by cyclopamine at 6 mg/ml significantly attenuates inflammatory cell accumulation and concomitantly reduces goblet cell metaplasia, cyclopamine at 1 mg/ml significantly attenuates goblet cell metaplasia but not inflammatory cell accumulation; this suggests that SHH contributes to goblet cell metaplasia through the direct activation of HH signaling, rather than inflammatory signaling. In addition, infection with either GFP-expressing or Cre-expressing adenoviruses in OVA-challenged bronchial epithelia causes no significant difference in the number of each inflammatory cell types, and this suggests that the observed difference in goblet cell metaplasia after GFP-expressing and Cre-expressing adenovirus infection should result from the Cre-mediated specific disruption of SMO in bronchial epithelia. Notably, cyclopamine blocks the goblet cell metaplasia as potently as SHH-Nab at 2.0 μg/mouse, but attenuates allergen-induced eosinophil accumulation less potently than SHH-Nab at 2.0 μg/mouse. The difference between cyclopamine and SHH-Nab on inflammatory cell infiltration can be explained by previous finding showing that SHH acts as a macrophage chemoattractant during the immune response.[33,34]

The transcription factor gene *FoxA2* is not only a direct target of the HH/GLI signaling cascade but a negative regulator for columnar metaplasia in allergic airway diseases.[35,36] Although *FoxA2* also serves as a direct target of HH signaling, FOXA2 positively regulates esophageal Barrett's metaplasia.[37] The discrepancy could indicate that the role of FOXA2 in HH signaling depends on the cell type involved. Consistent with our data that indicate that FOXA2 and SPDEF sever as negative and positive effectors of SHH signaling, respectively, in regulation of goblet cell metaplasia in the allergic airway, the expression of a *FoxA2* transgene markedly reduced allergen-induced mucous metaplasia in mice, whereas the disruption of *FoxA2* in respiratory epithelial cells caused airspace enlargement, neutrophilic pulmonary infiltrates, and mucous metaplasia.[7,32] On the other hand, SPDEF plays a positive role in goblet cell metaplasia and mucous hypersecretion, and the disruption of *Spdef* results in the absence of goblet cells in the conducting airway epithelia following allergen exposure.[6,9,38] Consistent with these findings, the present study not only confirms that GLI2 binds to the promoter region of the *Muc5AC* gene and induces the transcription of *Muc5AC*, but also identifies that SHH suppresses the expression of FOXA2 while also induces the expression of SPDEF; this corresponds their roles in goblet cell metaplasia and hypersecretion.[39]

Goblet cell metaplasia and resultant mucous hypersecretion are most striking characteristics in inflammatory airway diseases.[40] The high expression of SHH in allergic bronchial epithelia has a significant implication in goblet cell metaplasia and mucous hypersecretion of asthma, and hedgehog-interacting protein tatgeting bronchial epithelia is a COPD susceptibility gene that closely relates to the lung function of asthmatic patients.[41]

Therefore, we suggest that the study of the function of SHH signaling in mice is relevant to many common human diseases. Taking advantage of the openness of lung, the blockage of SHH signaling pathway in bronchial epithelia by virtue of the aerosol inhalation of SHH-Nab or HH pathway inhibitors is a promising therapeutic intervention for goblet cell metaplasia and mucous hypersecretion, the important causes of morbidity and mortality in chronic airway diseases.

METHODS

Children with FBA or allergic asthma

Children with a suspected diagnosis of FBA, tuberculosis, or bronchomalacia received diagnostic fiberoptic bronchoscopy with broncho-alveolar lavage (BAL). The current study used the remnant BALFs from four children (5–8 years old) with a discharged diagnosis of FBA and seven children (4–8 years old) with a discharged diagnosis of allergic asthma. Asthmatic children satisfied the American Thoracic Society criteria for asthma, including proven reactivity to skin allergen prick tests; they were characterized using spirometry and current symptom levels. All children with FBA, previously healthy, presented with a history of FBA 6 h before admission; bronchoscopy found food, bone and rock in the bronchi, and the foreign bodies were successfully extracted. The clinical characteristics of children with asthma and FBA were described in detail (Supplementary Table 1). All children underwent bronchoscopy as described previously, and received no medication before admission.[42] The BALFs were subjected to preparation of the cytospins and supernatants. The cytopsins were further subjected to Wright-Giemsa staining and immunofluorescent staining for Club cell 10-kDa protein (CC10, sc365992, Santa Cruz Biotechnology, Inc., Santa Cruz, CA), and SHH (06-1106, Millipore, Billerica, MA), whereas the supernatants were stored at −80 °C until further ELISA assays for N-SHH (DSHH00, R&D Systems, Inc., Minneapolis, MN) and Bradford assays for protein quantification (Beyotime, Shanghai, China) were undertaken. The use of remnant BALFs in the present study was approved by the Clinical Research Ethics Committee of the Children's Hospital at the Zhejiang University School of Medicine. Written consent for diagnostic fiberoptic bronchoscopy with BAL, as well as written consent for the use in research of remnant BALFs, was obtained from the children's guardians, with no financial incentive provided.

Mouse strains

C57BL/6J mice at 8-week-old were purchased from Shanghai SLAC Laboratory Animal Co. Ltd. (Shanghai, China), and *SMO*$^{flox/flox}$ and *R26-SMO-M2* mouse strains were obtained from the Jackson Laboratory (Bar Harbor, ME) and generated as previously described.[43, 44] All animals were housed and bred at the Zhejiang University Animal Care Facility according to the institutional guidelines for laboratory animals, and the protocol was approved by the Zhejiang University Institutional Animal Care and Use Committee.

Mouse models with allergen-induced allergic airway diseases

OVA-induced mouse models with asthma were prepared as described previously.[45] Briefly, all mice were sensitized via subcutaneous injection with 20 μg/mouse of OVA (Sigma, St. Louis, MO) emulsified in 2 mg aluminum hydroxide adjuvant at footpad, neck, back, and groin, on day 0 and 10. From day 19, the *SMO*$^{flox/flox}$ and *R26-SMO-M2* mice were intratracheally instilled with green fluorescent protein (GFP-Ad)-expressing or Cre recombinase (Cre-Ad)-expressing adenoviruses, once daily for 3 days,[45] whereas the wild-type mice were kept intact. From day 22 to 28 (day 22–24 for *R26-SMO-M2* mice), the sensitized mice were aerosolized with 1% OVA or an equal volume of 0.1 M PBS by a jet nebulizer (BARI Co. Ltd., Germany) for 30 min, once daily. In some cases, 2 h after each OVA aerosol, wild-type mice were intratracheally administered with either 50 μl/mouse mouse N-SHH neutralizing antibody (MAB4641, R&D) or IgG (MAB006, R&D) at 10 and 40 μg/ml in the presence or absence of mouse serum albumin (Sigma) or recombinant mouse N-SHH protein (rmN-SHH, #461-SH, R&D Systems). Alternatively, 2 h after each OVA aerosol, wild-type mice were aerosolized with 5 ml of cyclopamine solution (Sigma) at 1 and 6 mg/ml or same volume of solvent for 15 min, once daily for 7 days. HDM-induced mouse models with allergic airway disease were prepared as previously described.[25, 46] Briefly, mice were intranasally administered either 10 μg (10 μl of 1 mg/ml protein weight solution in normal saline) HDM extract (Greer Laboratories, Lenoir, NC) or a same volume of normal saline for 10 days; after 3 weeks, mice further intranasally received 10 μg HDM, once daily for 3 days, to trigger recall responses.

Detection of SMO expression in eosinophils, mesenchymal stromal cells, and Club cells from lung of *SMO*$^{flox/flox}$ mice

The sensitized *SMO*$^{flox/flox}$ mice were intratracheally instilled with GFP-Ad-expressing or Cre-Ad-expressing adenoviruses, once daily for 3 days, then, the mice were aerosolized with 1% OVA for 30 min, once daily for 7 days. Twenty-four hours after the last OVA challenge, lungs were harvested and a single-cell suspension was prepared by using a mouse Lung Dissociation Kit (Miltenyi Biotec Inc., Auburn, CA) as previously described.[47] The single-cell suspension was used for immunofluorescent staining of SMO, C-C chemokine receptor type 3 (CCR3, an eosinophil marker), vimentin (a mesenchymal stromal cell marker), CC10 (a Club cell marker).

Cell counting and classification in BALFs

BALFs were prepared as previously described.[45, 48] Briefly, 24 h after the last OVA challenge, mice were anesthetized with urethane (2 g/kg, i.p.), and BALFs were then obtained via tracheal tube. BALFs were centrifuged and the pellets were resuspended with Hank's balanced salt solution for cell count, Wright-Giemsa staining and classification.

H&E and PAS staining and immunostaining

Histological examination was performed as previously described.[26, 48] Briefly, lungs were infused via trachea with 1 ml of 10% neutralized formalin for 7 days. After tissues were paraffinized, 5-μm sections were subjected to H&E and PAS stains. PAS staining was performed by using PAS kit (Sigma). Immunohistochemistry staining was performed by using the Histostain-Plus Kit (Kangwei Reagents, Beijing, China) as described previously.[10] Primary antibodies against DHH (SC-271168, Santa Cruz Biotechnology), IHH (ab39634, Abcam, Cambridge, UK), SHH (06-1106, Millipore), PTCH1 (06-1102, Millipore), and SMO (ab72130, Abcam) were incubated at 4 °C overnight. Immunofluorescence staining was performed as described previously.[49] The antibodies used were as follows: CCR3 (ab36827, Abcam), vimentin (sc26002, Santa Cruz Biotechnology), CC10 (sc365992, Santa Cruz Biotechnology), MUC5AC (ab3649, Abcam), SPDEF (ab197375, Abcam), FOXA2 (Santa Cruz Biotechnology), Alexa555 or Alexa488-conjugated secondary antibody (Invitrogen, Grand Island, NY). Semi-quantitative histomorphometry for PAS, immunohistochemistry, and immunofluorescence staining was performed blindly in 10 different fields for each lung section by using Image-Pro Plus 6.0 software (Media Cybernetics, Silver Spring, MD) as previously described.[50] Briefly, 10 digital images at 1360 × 1024 pixel resolution and 400× magnification were captured by a DP 70 CCD camera (Olympus, Japan) coupled to an Olympus AX-70 microscope (Olympus). The measurement parameters included density mean, area sum, and integrated optical density (IOD). The optical density was calibrated and the area of interest was set through: hue, 0–30; saturation, 0–255; intensity, 0–255, then the image was converted to gray scale image, and the values were

counted. The area sum and IOD were log10 transformed. Relative index of staining was calculated using the following formula: Relative index = $\log10^{\text{area sum}} \times \log10^{\text{IOD}}$. Mean indexes were derived from 6 mice with 60 different fields.

Cell cultures and treatments

Human bronchial epithelial cells, 16HBE cells (a differentiated SV-40 transformed bronchial epithelial cell line) were generously gifted from Professor Huahao Shen from Zhejiang University and grew in minimal essential medium with Earle's salts (Life Technologies, Carlsbad, California) supplemented with 10% fetal calf serum (Life Technologies). The cells were subcultured before reaching confluence and incubated at 37 °C with 5% CO_2. After pre-culture for 24 h, cells were treated with indicated concentrations of purmophamine or bioactive recombinant human SHH (N-SHH, 1845-SH, R&D Systems) for 24 h. Then, cells were subjected to preparation of total RNA and protein lysates for quantitative RT-PCR and western blots, respectively. In some cases, cells were infected with scramble-expressing, GLI1-expressing, or GLI2-shRNA-expressing lentiviruses for 24 h, before treated with purmorphamine.

Generation of lentiviruses expressing GLI1-shRNA or GLI2-shRNA

Lentiviruses expressing either GLI1-shRNA or GLI2-shRNA were generated as previously described.[49] The hairpin shRNA templates of complementary oligonucleotide containing overhangs were digested, and the synthesized complementary oligonucleotides for GLI1-shRNA and GLI2-shRNA were annealed and inserted into the pSicor vector. The shRNA-expressing lentiviral vector was co-transfected with plasmids pLP1, pLP2 and vsvg into 293T cells. Virus-containing media were collected and filtered. Knockdown was confirmed by two or more unrelated shRNA constructs.

Western blots and quantitative RT-PCR

Total protein extracts from lungs or 16HBE cells were prepared in whole cell lysis buffer as described previously.[49] Protein were resolved on 10% polyacrylamide gel, transferred onto a 0.45 μm PVDF membrane (Millipore), and detected with specific antibodies: SHH (06-1106, Millipore), SMO (ab72130, Abcam), FOXA2 (SC-20687, Santa Cruz), SPDEF (ab26056, Abcam), and β-actin (SC-69879, Santa Cruz). National Institutes of Health Image software (ImageJ, http://rsb.info.nih.gov/ij/) was used to quantify the immunoreactive bands, and the normalized antigen signals were calculated from target protein-derived and β-actin-derived signals. The mean density of first bands was set to 1. Total RNA was isolated by using a TRIzol reagent (Takara Biotechnology Co., Ltd., Dalian, China) according to the manufacturer's instructions. 5 μg total RNA was reversely transcribed by using SuperScript III reagent (Life Technologies). Messenger RNA levels of target genes were determined by RT-PCR and qPCR as previously described.[49] The primer pairs for the genes analyzed by quantitative RT-PCR were described in detail (Supplementary Table 2).

Transient transfection and reporter assays

Human *Muc5AC* gene promoter region (nt−1300/+48) was amplified by PCR in the presence of genomic DNA from 16HBE cells.[14] The primers were as follows: Forward: 5′-AGAGCTTGG GACGGGTCC-3′ and Reverse: 5′-GTGTGTGGACGGCGGGGAAGA-3′. The PCR products were cloned into pGL3-Basic vector (Promega, Madison, WI) to generate the luciferase reporter constructs of *Muc5AC* gene. Transient transfection was performed by using Lipofectamine 2000 as per the manufacturer's instruction. The cells were then either cultured in the presence or absence of purmophamine or N-SHH recombinant protein for 36 h. Cell lysates were prepared in 100 μl reporter lysis buffer (Promega), and 20 μl supernatants of cellular lysate were used for dual-luciferase assay according to the manufacturer's instructions (Promega). The firefly luciferase levels were normalized to Renilla luciferase levels, the first bar was defined as 1.

Chromatin immunoprecipitation (ChIP) assays

ChIP was performed by using a commercial EpiQuikChIP kit (QWBio, Beijing, China) according to the manufacturer's instruction.[49] Briefly, cells were fixed with formaldehyde to cross-link the transcription factors to chromatin DNA. After washing with PBS, cells were re-suspended with lysis buffer supplemented with protease inhibitor cocktail. The shearing of chromatin DNA for producing an approximately 500 bp of input DNA was performed by sonication, and subjected to immunoprecipitation with negative control IgG, or GLI2 antibody (ab26056, Abcam). After the immunoprecipitates were incubated with protein A agarose/salmon sperm DNA (Santa Cruz), the antibody–protein–DNA–agarose complex was washed and harvested for subsequent reverse cross-linking. The sheared DNA fragments from reverse cross-linking were extracted with a DNA extraction kit for PCR amplification as previously described.[49] The primers 5′-CTCGGAAACTGGGCTCTACCCGG-3′ and 5′-GAGCTTTTTGTAGCCCCAGAGCTGG-3′ were used to amplify a fragment of the *Muc5AC* promoter region.[39]

Statistical analysis

Numerical data are expressed as mean ± SEM from six mice or four independent cultures. Statistical calculations were performed using SigmaStat software (SigmaStat 2.0, SPSS Inc., Chicago, IL, USA). Significance was evaluated by one-way ANOVA and Tukey–Kramer multiple comparisons test. Statistical significance was assessed at levels of $p < 0.05$ and $p < 0.01$. Experiments were repeated three times with similar results, and representative results were shown.

ACKNOWLEDGEMENTS

This work is supported by National Natural Science Foundation of China (Nos. 81470214, 81170016, 81170787, 81200022, 81200023, 81270067, 31571493, and 81571928) and NIH (R01 DK 065789 to F.L.).

AUTHOR CONTRIBUTIONS

C.C.Z., Q.M.X., Y.K., L.F.T., and X.M.W. were the main contributors in the conception, design, acquisition, and interpretation of the data and in writing the article. C.Y.X., M. H., Y.N.S., W.S., Z.Y.J., and X.L.W. performed experiments and data analysis. M.P.L. and J.S.W. interpreted histopathology. M.H. and Y.N.S. were responsible for image analysis. L.F.T. and X.M.W. wrote the paper.

ADDITIONAL INFORMATION

The online version of this article (https://doi.org/10.1038/s41385-018-0033-4) contains supplementary material, which is available to authorized users.

Competing interests: The authors declare no competing interests.

Publisher's note: Springer Nature remains neutral with regard to jurisdictional claims in published maps and institutional affiliations.

REFERENCES

1. Curran, D. R. & Cohn, L. Advances in mucous cell metaplasia: a plug for mucus as a therapeutic focus in chronic airway disease. *Am. J. Respir. Cell Mol. Biol.* **42**, 268–275 (2010).
2. Rock, J. R. & Hogan, B. L. Epithelial progenitor cells in lung development, maintenance, repair, and disease. *Annu. Rev. Cell Dev. Biol.* **27**, 493–512 (2011).
3. Tyner, J. W. et al. Blocking airway mucous cell metaplasia by inhibiting EGFR antiapoptosis and IL-13 transdifferentiation signals. *J. Clin. Invest.* **116**, 309–321 (2006).
4. Matsukura, S. et al. Interleukin-13 upregulates eotaxin expression in airway epithelial cells by a STAT6-dependent mechanism. *Am. J. Respir. R. Cell Mol. Biol.* **24**, 755–761 (2001).
5. Kuperman, D. A. et al. Direct effects of interleukin-13 on epithelial cells cause airway hyperreactivity and mucus overproduction in asthma. *Nat. Med.* **8**, 885–889 (2002).

6. Park, K. S. et al. SPDEF regulates goblet cell hyperplasia in the airway epithelium. *J. Clin. Invest.* **117**, 978–988 (2007).
7. Wan, H. et al. Foxa2 regulates alveolarization and goblet cell hyperplasia. *Development* **131**, 953–964 (2004).
8. Kistemaker, L. E. et al. Tiotropium attenuates IL-13-induced goblet cell metaplasia of human airway epithelial cells. *Thorax* **70**, 668–676 (2015).
9. Chen, G. et al. SPDEF is required for mouse pulmonary goblet cell differentiation and regulates a network of genes associated with mucus production. *J. Clin. Invest.* **119**, 2914–2924 (2009).
10. Pan, Y. B. et al. Sonic hedgehog through Gli2 and Gli3 is required for the proper development of placental labyrinth. *Cell Death Dis.* **6**, e1653 (2015).
11. Robbins, D. J., Fei, D. L. & Riobo, N. A. The hedgehog signal transduction network. *Sci. Signal* **5**, re6 (2012).
12. Briscoe, J. & Therond, P. P. The mechanisms of hedgehog signalling and its roles in development and disease. *Nat. Rev. Mol. Cell Biol.* **14**, 416–429 (2013).
13. Pepicelli, C. V., Lewis, P. M. & McMahon, A. P. Sonic hedgehog regulates branching morphogenesis in the mammalian lung. *Curr. Biol.* **8**, 1083–1086 (1998).
14. Bellusci, S. et al. Involvement of Sonic hedgehog (Shh) in mouse embryonic lung growth and morphogenesis. *Development* **124**, 53–63 (1997).
15. Litingtung, Y., Lei, L., Westphal, H. & Chiang, C. Sonic hedgehog is essential to foregut development. *Nat. Genet.* **20**, 58–61 (1998).
16. Peng, T. et al. Hedgehog actively maintains adult lung quiescence and regulates repair and regeneration. *Nature* **526**, 578–582 (2015).
17. Miller, L. A., Wert, S. E. & Whitsett, J. A. Immunolocalization of sonic hedgehog (Shh) in developing mouse lung. *J. Histochem. Cytochem.* **49**, 1593–1604 (2001).
18. Zhang, M., Wang, H., Teng, H., Shi, J. & Zhang, Y. Expression of SHH signaling pathway components in the developing human lung. *Histochem. Cell Biol.* **134**, 327–335 (2010).
19. Watkins, D. N. et al. Hedgehog signalling within airway epithelial progenitors and in small-cell lung cancer. *Nature* **422**, 313–317 (2003).
20. Miller, L. A. et al. Role of Sonic hedgehog in patterning of tracheal-bronchial cartilage and the peripheral lung. *Dev. Dyn.* **231**, 57–71 (2004).
21. Stewart, G. A. et al. Expression of the developmental Sonic hedgehog (Shh) signalling pathway is up-regulated in chronic lung fibrosis and the Shh receptor patched 1 is present in circulating T lymphocytes. *J. Pathol.* **199**, 488–495 (2003).
22. Fisher, C. E., Ahmad, S. A., Fitch, P. M., Lamb, J. R. & Howie, S. E. FITC-induced murine pulmonary inflammation: CC10 up-regulation and concurrent Shh expression. *Cell Biol. Int.* **29**, 868–876 (2005).
23. Furmanski, A. L. et al. Tissue-derived hedgehog proteins modulate Th differentiation and disease. *J. Immunol.* **190**, 2641–2649 (2013).
24. Kugler, M. C., Joyner, A. L., Loomis, C. A. & Munger, J. S. Sonic hedgehog signaling in the lung. From development to disease. *Am. J. Respir. Cell Mol. Biol.* **52**, 1–13 (2015).
25. Standing, A. S., Yanez, D. C., Ross, R., Crompton, T. & Furmanski, A. L. Frontline Science: Shh production and Gli signaling is activated in vivo in lung, enhancing the Th2 response during a murine model of allergic asthma. *J. Leukoc. Biol.* **102**, 965–976 (2017).
26. Whitsett, J. A., Haitchi, H. M. & Maeda, Y. Intersections between pulmonary development and disease. *Am. J. Respir. Crit. Care Med.* **184**, 401–406 (2011).
27. Tang, C. et al. Hedgehog signaling stimulates the conversion of cholesterol to steroids. *Cell Signal* **27**, 487–497 (2015).
28. Nakashima, H. et al. Nuclear factor-kappaB contributes to hedgehog signaling pathway activation through sonic hedgehog induction in pancreatic cancer. *Cancer Res.* **66**, 7041–7049 (2006).
29. Schuliga, M. NF-kappaB signaling in chronic inflammatory airway disease. *Biomolecules* **5**, 1266–1283 (2015).
30. Grunig, G. et al. Requirement for IL-13 independently of IL-4 in experimental asthma. *Science* **282**, 2261–2263 (1998).
31. Temann, U. A., Geba, G. P., Rankin, J. A. & Flavell, R. A. Expression of interleukin 9 in the lungs of transgenic mice causes airway inflammation, mast cell hyperplasia, and bronchial hyperresponsiveness. *J. Exp. Med.* **188**, 1307–1320 (1998).
32. Zhu, Z. et al. Pulmonary expression of interleukin-13 causes inflammation, mucus hypersecretion, subepithelial fibrosis, physiologic abnormalities, and eotaxin production. *J. Clin. Invest.* **103**, 779–788 (1999).
33. Dunaeva, M., Voo, S., van Oosterhoud, C. & Waltenberger, J. Sonic hedgehog is a potent chemoattractant for human monocytes: diabetes mellitus inhibits Sonic hedgehog-induced monocyte chemotaxis. *Basic Res. Cardiol.* **105**, 61–71 (2010).
34. Schumacher, M. A. et al. Gastric Sonic hedgehog acts as a macrophage chemoattractant during the immune response to Helicobacter pylori. *Gastroenterology* **142**, 1150–1159 (2012).
35. Park, S. W. et al. Distinct roles of FOXA2 and FOXA3 in allergic airway disease and asthma. *Am. J. Respir. Crit. Care Med.* **180**, 603–610 (2009).
36. Mavromatakis, Y. E. et al. Foxa1 and Foxa2 positively and negatively regulate Shh signalling to specify ventral midbrain progenitor identity. *Mech. Dev.* **128**, 90–103 (2011).
37. Wang, D. H. et al. Hedgehog signaling regulates FOXA2 in esophageal embryogenesis and Barrett's metaplasia. *J. Clin. Invest.* **124**, 3767–3780 (2014).
38. Kageyama-Yahara, N. et al. Gli regulates MUC5AC transcription in human gastrointestinal cells. *PLoS ONE* **9**, e106106 (2014).
39. Rajavelu, P. et al. Airway epithelial SPDEF integrates goblet cell differentiation and pulmonary Th2 inflammation. *J. Clin. Invest.* **125**, 2021–2031 (2015).
40. Holtzman, M. J., Byer, D. E., Alexander-Brett, J. & Wang, X. The role of airway epithelial cells and innate immune cells in chronic respiratory disease. *Nat. Rev. Immunol.* **14**, 686–698 (2014).
41. Li, X. et al. Importance of hedgehog interacting protein and other lung function genes in asthma. *J. Allergy Clin. Immunol.* **27**, 1457–1465 (2011).
42. Tang, L. F. et al. Airway foreign body removal by flexible bronchoscopy: experience with 1027 children during 2000-2008. *World J. Pediatr.* **5**, 191–195 (2009).
43. Zhang, X. M., Ramalho-Santos, M. & McMahon, A. P. Smoothened mutants reveal redundant roles for Shh and Ihh signaling including regulation of L/R symmetry by the mouse node. *Cell* **106**, 781–792 (2001).
44. Jeong, J., Mao, J., Tenzen, T., Kottmann, A. H. & McMahon, A. P. Hedgehog signaling in the neural crest cells regulates the patterning and growth of facial primordia. *Genes Dev.* **18**, 937–951 (2004).
45. Qin, X. J. et al. Protein tyrosine phosphatase SHP2 regulates TGF-beta1 production in airway epithelia and asthmatic airway remodeling in mice. *Allergy* **67**, 1547–1556 (2012).
46. Lu, M. et al. Therapeutic induction of tolerance by IL-10-differentiated dendritic cells in a mouse model of house dust mite-asthma. *Allergy* **66**, 612–620 (2011).
47. Gadepalli, V. S., Vaughan, C. & Rao, R. R. Isolation and characterization of murine multipotent lung stem cells. *Methods Mol. Biol.* **962**, 183–191 (2013).
48. Yao, H. Y. et al. Inhibition of Rac activity alleviates lipopolysaccharide-induced acute pulmonary injury in mice. *Biochim. Biophys. Acta* **1810**, 666–674 (2011).
49. Tang, C. et al. Glioma-associated oncogene 2 is essential for trophoblastic fusion by forming a transcriptional complex with glial cell missing-a. *J. Biol. Chem.* **291**, 5611–5622 (2016).
50. Wang, C. J. et al. Survivin expression quantified by Image Pro-Plus compared with visual assessment. *Appl. Immunohistochem. Mol. Morphol.* **17**, 530–535 (2009).